J. Chosun Natural Sci.
Vol. 9, No. 4 (2016) pp. 223 – 227
https://doi.org/10.13160/ricns.2016.9.4.223

Fabrication of ZnSn Thin Films Obtained by RF co-sputtering

Seokhee Lee, Juyun Park, Yujin Kang, Ahrom Choi, Jinhee Choi, and Yong-Cheol Kang†

Abstract

The Zn, Sn, and ZnSn thin films were deposited on Si(100) substrate using radio frequency (RF) magnetron co-sputtering method. A surface profiler and X-ray photoelectron spectroscopy (XPS) were used to investigate the Zn, Sn, and ZnSn thin films. Thickness of the thin films was measured by a surface profiler. The deposition rates of pure Zn and Sn thin films were calculated with thickness and sputtering time for optimization. From the survey XPS spectra, we could conclude that the thin films were successfully deposited on Si(100) substrate. The chemical environment of the Zn and Sn was monitored with high resolution XPS spectra in the binding energy regions of Zn 2p, Sn 3d, O 1s, and C 1s.

Keywords: Zinc Oxide, X-ray Photoelectron Sectroscopy, Thin Films

1. Introduction

Zinc oxide (ZnO) is a typical II-VI group oxide semiconducting material that has a band gap energy of 3.37 eV[1]. ZnO material system shows chemical and thermal stability at room temperature. Also, it has been actively studied for various applications such as photoelectric devices, solar cells, UV sensors, and piezoelectric devices due to its large free exciton binding energy and ease of control the electronic conductivity[1,2]. Tin oxide (SnO) applied for p-type semiconductor has a large electronic conductivity due to 5s orbital structure of Sn in valence band maximum. SnO has been attracting immense attention as transparent devices such as thin films transistor[3]. When the zinc tin oxide (ZTO) was synthesized using Zn and Sn, it showed the reduction of significant oxygen vacancy[4]. It could be applied in channel layer because of the low resistance and high transmittance[5-7].

ZTO thin films could be fabricated with various methods such as pulsed laser deposition[8], chemical vapor deposition[9], sol-gel[10], spray pyrolysis[11], and sputtering method[12]. Sputtering methods are divided into two categories in accordance with the kinds of applying power on the target. One is the direct current (DC) sputtering method using direct current and the other is the radio frequency (RF) sputtering method using high frequency of radio wave with alternating voltage. The advantage of RF sputtering method is that it could be apply for both insulators and conductors while DC sputtering is applicable to conductors only.

Before investigating the ZTO films, we fabricated the Zn, Sn, and ZnSn thin films to study metallic films excluding oxygen gas effect. We calculated the deposition rates of pure Zn and Sn thin films at various RF sputter powers using a surface profiler, and then we controlled the compositional ratios of Zn to Sn in the thin films using deposition rates. To analyze the chemical environment and the atomic ratio, X-ray photoelectron spectroscopy (XPS) was used.

2. Experimental Section

Thin films (Zn, Sn, and ZnSn) were fabricated by RF co-sputtering method in the ultrahigh vacuum (UHV) chamber on p-type Si(100) substrate. The schematic diagram of UHV RF co-sputtering chamber are shown in Fig. 1.

The metallic Zn and Sn targets (99.99%, Vacuum Thin Film Materials, Korea) were used in this work. The base pressure of the UHV chamber was maintained about 1.33×10^{-6} Pa by using a turbo molecular pump (TMP) backed by a rotary vane pump (RP). The sub-

Department of Chemistry, Pukyong National University, 45, Yongso-ro, Nam-Gu, Busan, 48513, Korea

†Corresponding author : yckang@pknu.ac.kr
(Received : August 20, 2016, Revised : December 17, 2016
Accepted : December 25, 2016)

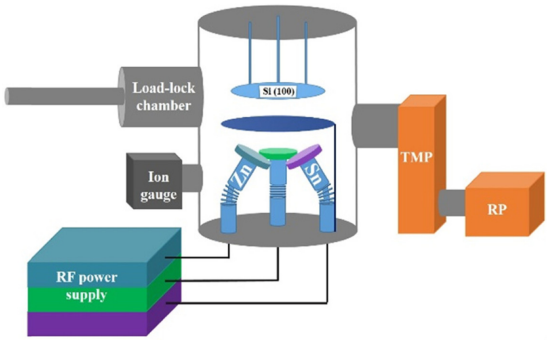

Fig. 1. The schematic diagram of ultra-high vacuum RF sputter chamber.

strate, p-type Si(100), was cleaned with acetone before loading in the UHV chamber. The substrate was rotated by 5 rpm during sputtering process to deposit uniformly on the whole area of substrate. Pure Ar gas was used as a sputter gas and the flow rate was kept at 20 sccm (standard cubic centimeters per minute, cm^3/min). Pre-sputtering process was conducted as the substrate was covered with a shutter before sputtering process. It could eliminate contaminants at the surface region of the targets and stabilize the plasma. Pre-sputtering process was performed at about 5.33 Pa of working pressure for 4 min and 20 W of RF power on the metal targets (Zn and Sn). And then, shutter was opened in order to start sputtering process for deposition. At that time, the pressure of the UHV chamber was kept about 1.33 Pa and the metallic targets were energized with various RF sputter powers from 10 to 40 W for 5 min. The UHV chamber was retained at 287 K using a chiller during sputtering process to exclude thermal effect on the metallic targets. Sample notation was decided according to the metal elements of thin films, that such as Zn, Sn, and ZnSn thin films.

The thickness of deposited thin films was measured using a surface profiler (Alpha-step 500, Tencor, USA) to calculate deposition rates of thin films. Then XPS (ESCALab MKII, VG, UK) with Mg Kα X-ray source (1253.6 eV) was performed for analysis of the chemical states of the elements.

3. Results and Discussion

Before fabrication of ZnSn thin films, we calculated deposition rates of pure metallic Zn and Sn thin films

Table 1. The thickness and deposition rate according to RF sputter power of Zn and Sn targets.

Target	RF power (W)	Thickness (nm)	Deposition rate (nm/min)
Zn	10	81.5	16.3
	14	156.9	31.4
	20	257.2	51.4
	30	392.1	78.4
Sn	10	22.4	4.5
	20	60.3	12.1
	30	121.3	24.3
	40	141.1	28.2

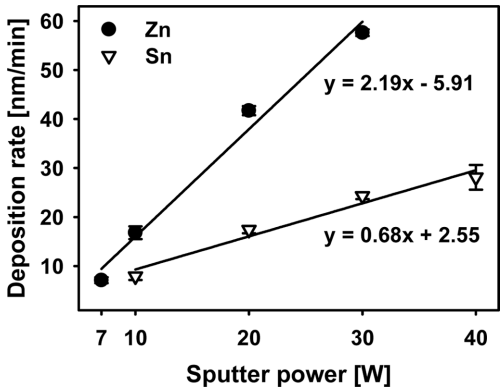

Fig. 2. The deposition rates of Zn and Sn thin films.

in order to control the relative atomic ratio Zn to Sn in the ZnSn thin films. The thickness and deposition rates of the thin films as a function of RF sputter power on each metal target are listed in Table 1.

The deposition rates was calculated using the thickness and sputtering time. In the Fig. 2, x is the RF power applied on the targets and y is the deposition rates of the Zn and Sn films. Fig. 2 shows the deposition rates of Zn and Sn with increasing RF sputter power on Zn and Sn targets. As we expected, as the RF power increased, the thickness of the thin films increased. The deposition rate of Zn was higher than Sn as shown in Fig. 2. When we compare the melting points of the Zn (693 K) and Sn (505 K), we expected that deposition of Sn was higher than Zn.

Interestingly, the opposite propensity was observed. Increase of deposition rates was proportional to the applied RF sputter power on each metal target. The RF sputter power for each target was selected where that

showed the same deposition rates for the formation of metallic mixture of Zn and Sn. As a result, the selected RF powers for 24 nm/min of deposition rate were 12 and 30 W for Zn and Sn targets, respectively. Thus, we fabricated ZnSn thin film applied the selected RF sputter powers on each target.

Fig. 3 shows the XPS survey spectra of Zn, Sn, and ZnSn thin films obtained by RF co-sputtering method. ZnSn thin film was fabricated by applying 12 and 30 W of RF sputter powers on Zn and Sn targets, respectively. Pure Zn and Sn thin films were fabricated with 14 W for Zn and 30 W for Sn of RF powers.

The characteristic peaks in the binding energy regions of from 1014 to 1052 eV for Zn 2p and in the binding energy regions of from 478 to 501 eV for Sn 3d were distinctly observed. This implies that ZnSn film was successfully deposited on Si(100) substrate. Another XPS peaks corresponded to O 1s and C 1s were also observed and broad peaks assigned to Auger peaks such as Zn LMM (265~429 eV), Sn MNN (819~827 eV), and O KLL (nearby 743 eV) were evolved in ZnSn thin films as shown in Fig. 3. The notation of Auger peaks is related with the sequence of the hole generated in the electronic shell. Which was explained by following steps; in case of Zn, first, electron of core level (L) was ejected by X-ray radiation. Second, the electron of upper core level (M) was transferred to hole to relax the system. Third, the energy due to the transition from M to L could eject another electron in other shell (M). Due to the exposure of the obtained films in atmospheric environment during transferring from RF co-sputter chamber to XPS analysis chamber, the thin films could be contaminated by air. Adsorption of water and carbon dioxide molecules on the thin films causing O and C peaks.

Unexpectedly, the Zn 2p XPS peak was evolved at the survey XPS spectra of Sn thin film as shown in the bottom spectra in Fig. 3. This implies that the Sn target was contaminated Zn during co-sputtering process. This problem was solved by cleaning the surface of Sn target with long pre-sputtering process.

The high resolution Zn 2p and Sn 3d XPS spectra were measured as shown in Fig. 4 (a) and (b), respectively. The Zn 2p XPS peak was split into doublet with Zn $2p_{3/2}$ (1022.0 eV) and Zn $2p_{1/2}$ (1045.1 eV) peaks due to spin-orbit-splitting (SOS) as shown in Fig. 4(a). The interaction between spin angular momentum of the electron (up or down) and its orbital angular momentum causes splitting of the electron energy level. This is called SOS. The ratio of their multiplicity is signified as $2J+1$, thus J is the total angular momentum quantum number. Therefore, the multiplicity of Zn $2p_{1/2}$ is 2 and that of Zn $2p_{3/2}$ is 4. Because of the multiplicity of the peak, the peak intensity of Zn $2p_{3/2}$ is twice larger than that of Zn $2p_{1/2}$. The Sn 3d peaks were also resolved into doublet with Sn $3d_{5/2}$ and Sn $3d_{3/2}$ like the Zn 2p peak due to large SOS as shown in Fig. 4(b). In the same manner, multiplicities were 6 and 4 for $3d_{5/2}$ and $3d_{3/2}$, respectively. The peak intensity of Sn $3d_{5/2}$ was one and half times larger than that of Sn $3d_{3/2}$. But the peak splitting of Sn 3d could be appeared not only SOS but also the other reason at ZnSn thin film. One of the plausible reasons is that the different chemical states of

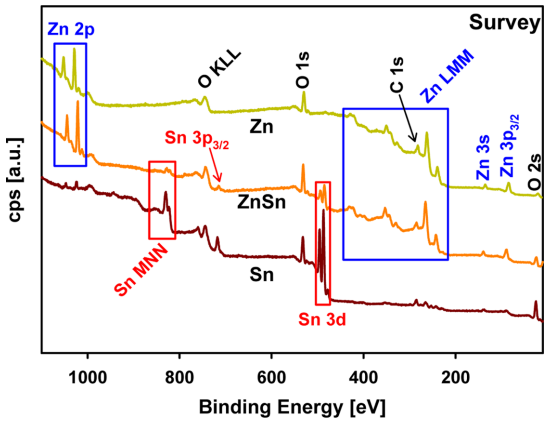

Fig. 3. The survey XPS spectra of ZnSn thin films.

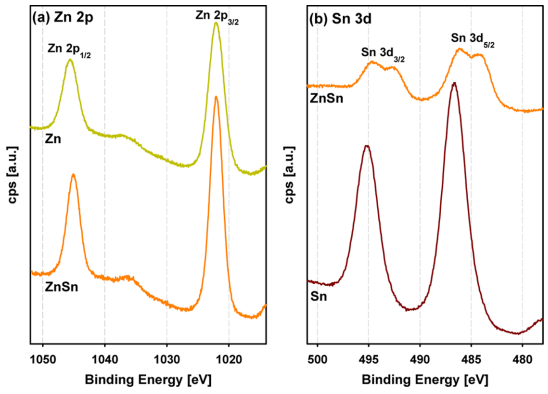

Fig. 4. The XPS narrow spectra of (a) Zn 2p and (b) Sn 3d.

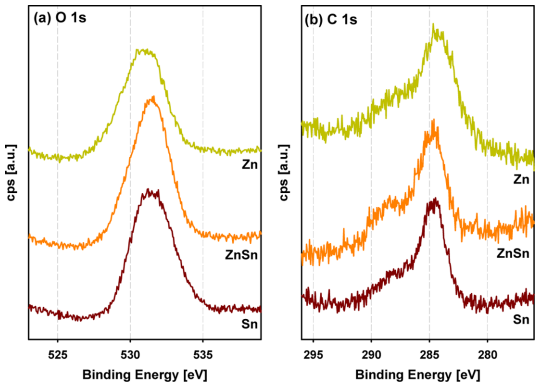

Fig. 5. XPS narrow spectra of (a) O 1s and (b) C 1s.

elements which existed in metallic Sn and oxidized Sn in ZnSn thin film. The oxidized Sn peak was evolved at high binding energy and the metallic Sn peak was appeared at low binding energy. Because the metallic Sn was electron richer than that of oxidized Sn. The electron rich environment reduced the binding energy of the photoelectron.

Fig. 5(a) and (b) were high resolution XPS spectra corresponded to O 1s and C 1s, respectively. In spite of the electron are delocalized in the same 1s orbital, the peak position of O 1s was higher binding energy than that of C 1s. The number of proton in O is larger than C that caused higher effective nuclear charge on O. This showed higher binding energy in O 1s than C. The peak intensities of O and C 1s were constant in all thin films due to contamination by exposure to atmosphere. The peak profiles of O 1s and C 1s were broad and had a shoulder, which demonstrated coexistence of various oxidation states.

4. Conclusion

We fabricated Zn, Sn, and ZnSn thin films by RF magnetron co-sputtering method in UHV chamber. Zn and Sn thin films were fabricated with various RF sputter powers from 10 to 40 W on pure metallic targets. The deposition rates of Zn and Sn were determined using the thickness of thin films and deposition time. Based on the determined deposition rates, the RF sputter powers were selected with the same 24 nm/min of deposition rates for 12 W on Zn and 30 W on Sn targets. We fabricated Zn, Sn, and ZnSn thin films using above condition. The characteristics of the obtained thin films were analyzed by XPS, we confirmed that the desired metals were properly deposited on Si(100) through XPS peaks and Auger peaks for each elements.

Acknowledgement

This work was supported by a Research Grant of Pukyong National University (2016 year: C-D-2016-0217)

References

[1] T. P. Rao and M. C. Santhoshkumar, “Effect of thickness on structural, optical and electrical properties of nanostructured ZnO thin films by spray pyrolysis”, Appl. Surf. Sci., Vol. 255, pp. 4579-4584, 2009.

[2] M.-B. Bouzourâa, A. En Naciri, A. Moadhen, H. Rinnert, M. Guendouz, Y. Battie, A. Chaillou, M.-A. Zaïbi, and M. Oueslati, “Effects of silicon porosity on physical properties of ZnO films”, Mater. Chem. Phys., Vol. 175, pp. 233-240, 2013.

[3] Y. Ogo, H. Hiramatsu, K. Nomura, H. Yanagi, T. Kamiya, M. Kimura, M. Hirano, and H. Hosono, “Tin monoxide as an s-orbital-based p-type oxide semiconductor: Electronic structures and TFT application”, Phys. Status Solidi A., Vol. 206, pp. 2187-2191, 2009.

[4] M.-Y. Tsai, W.-H. Cheng, J.-S. Jeng, and J.-S. Chen, “Improving performance of inverted organic solar cells using ZTO nanoparticles as cathode buffer layer”, Solid State Electron., Vol. 120, pp. 56-62, 2016.

[5] C.-X. Huang, J. Li, Y.-Z. Fu, J.-H. Zhang, X.-Y. Jiang, and Z.-L. Zhang, “Origin of the improved stability under negative gate-bias illumination stress in various sputtering power fabricated ZnSnO TFTs”, Superlattice. Microst., Vol. 88, pp. 426-433, 2015.

[6] Y.-Y. Choi, S. J. Kang, and H.-K. Kim, “Rapid thermal annealing effect on the characteristics of ZnS-nO_3 films prepared by RF magnetron sputtering”, Curr. Appl. Phys., Vol. 12, pp. S104-S107, 2012.

[7] Y. Nakanishi, K. Kato, M. Horikawa, and M. Yonekura, “Influence of Zn-Sn ratio on optical property and microstructure of Zn-Sn-O films deposited by magnetron sputtering”, Thin Solid Films, Vol. 612, pp. 231-236, 2016.

[8] J. H. Kim, K. A. Jeon, G. H. Kim, and S. Y. Lee, “Electrical, structural, and optical properties of ITO

thin films prepared at room temperature by pulsed laser deposition", Appl. Surf. Sci., Vol. 252, pp. 4834-4837, 2006.

[9] A. Salehi and M. Gholizade, "Gas-sensing properties of indium-doped SnO_2 thin films with variations in indium concentration", Sensor. Actuat. B-chem., Vol. 89, pp. 173-179, 2003.

[10] C. Terrier, J. P. Chatelon, and J. A. Roger, "Electrical and optical properties of Sb:SnO_2 thin films obtained by the sol-gel method", Thin Solid Films, Vol. 295, pp. 95-100, 1997.

[11] G. Turgut and E. Sönmez, "Synthesis and characterization of Mo doped SnO_2 thin films with spray pyrolysis" Superlattice. Microst., Vol. 69, pp. 175-186, 2014.

[12] Y. Hayashi, K. Kondo, K. Murai, T. Moriga, I. Nakabayashi, H. Fukumoto and K. Tominaga, "ZnO-SnO_2 transparent conductive films deposited by opposed target sputtering system of ZnO and SnO_2 targets", Vacuum, Vol. 74, pp. 607-611, 2004.